Mechanical characterization of OFE-Cu at low and high strain rates for SRF cavity fabrication by electro-hydraulic forming

J-F. Croteau[a], E. Cantergiani[a], N. Jacques[b], A.E.M. Malki[b], G. Mazars[c], G. Avrillaud[c]

a. I-Cube Research, Toulouse, France, jean-francois.croteau@icube-research.com

b. ENSTA Bretagne, UMR CNRS 6027, IRDL, Brest, France

c. Bmax, Toulouse, France

Résumé :

Pour le futur collisionneur circulaire (FCC) du CERN, la fabrication de cavités supraconductrices à radiofréquence (SRF) à haute performance est cruciale pour l'atteinte d'énergie de collision suffisante pour l'avancement de la recherche en physique des particules. Les cavités SRF, composantes responsables de l'accélération du faisceau de particules, sont fabriquées de niobium ou d'un substrat de cuivre revêtu de niobium. Pour assurer la croissance adéquate du film supraconducteur de niobium et prévenir la perte de la supraconductivité durant l'opération de l'accélérateur, les dommages sur la surface interne de la cavité de cuivre doivent être limités. Une alternative aux méthodes traditionnelles de formage, telles que l'emboutissage, le repoussage et l'hydroformage, est le formage électrohydraulique (EHF). En EHF, les demi-cellules sont fabriquées par une déformation rapide de la tôle en utilisant une onde de choc générée dans l'eau par une décharge électrique. Le design de procédés EHF requiert le développement de modèles multi-physiques numériques précis. Lors d'un formage en EHF, la matière est soumise à de hauts taux de déformation. Cette communication s'intéresse à la caractérisation mécanique à différents taux de déformation de cuivre électronique sans oxygène (OFE) recuit. La réponse en traction et compression du cuivre OFE est investiguée pour des taux entre $1x10^{-3}$ et $4x10^{3}$ s^{-1}. Les paramètres de l'équation constitutive Johnson-Cook ont été identifiés à partir des résultats expérimentaux à l'aide du logiciel d'éléments finis LS-DYNA, couplé au logiciel d'optimisation LS-OPT.

Abstract:

In the framework of CERN's Future Circular Collider (FCC), fabrication of high-performance superconducting radiofrequency (SRF) cavities is crucial to attain energy levels relevant for breakthrough research in particle physics. SRF cavities, the components responsible for beam acceleration, are made of bulk niobium or of a copper substrate with a niobium coating. To ensure proper growth of the niobium superconducting film and prevent quenching during operation, damage of the inner surface of copper cavities must be minimized. An alternative technique to traditional forming methods, such as deep-drawing, spinning, and hydroforming, is electro-hydraulic forming (EHF). In EHF, half-cells are formed through high-speed deformation of blanks, using shockwaves induced in water by a pulsed electrical discharge. The design of EHF processes requires the development of accurate, multi-physics numerical models. During an EHF operation, the material is subjected to high strain-rates. The proposed communication deals with the mechanical characterization of annealed

oxygen-free electronic (OFE) copper at different strain-rates. The constitutive response in tension and compression of OFE copper is investigated, for strain-rates ranging between $1x10^{-3}$ and $4x10^{3}$ s^{-1}. From the obtained experimental results, parameters for the Johnson-Cook constitutive model have been identified using the finite element software LS-DYNA, coupled with the optimization software LS-OPT.

Keywords: OFE copper, high strain-rate, electro-hydraulic forming, Johnson-Cook model, SRF cavity

1 Introduction

To reduce fabrication cost in large particle accelerators, such as the Large Hadron Collider (LHC), the European Organization for Nuclear Research (CERN) produces superconducting radiofrequency (SRF) cavities with a bulk copper structure, coated with a niobium superconducting layer (Nb/Cu cavities). The reduction in cost and energy consumption for similar performances makes Nb/Cu cavities a compelling choice for large accelerator projects. Multiple cavities at a resonance frequency of 400 and 800 MHz are needed [1], [2] for the construction of the Future Circular Collider (FCC), a new particle accelerator with 100 TeV and higher collision energies [3], a ten-fold increase compared to the LHC. In this regard, a thorough material characterization at low and high strain rates is essential for the development of accurate multi-physics finite element EHF models. Due to the high forming velocity nature of EHF, the sheet undergoes strain rates of up to 10^3-10^4 s^{-1}. Impacts of the blank on the die at 50 to 200 m/s also lead to compressive stresses in the thickness that needs to be modeled.

Fabrication of SRF cavities with electro-hydraulic forming (EHF) exhibits several advantages compared with traditional forming processes. Higher shape accuracy, increased formability, reduced surface roughness, reduced springback, and reduced contamination of the inner surface are reported benefits of EHF over deep-drawing, spinning, and hydroforming [4].

For high cavity performances, oxygen-free electronic (OFE) copper (ASTM C10100), a standardized copper with high purity and electrical conductivity, is used. According to ASTM standard B170-99, a minimum copper content of 99.99% is required and chemical impurities should follow the content presented in the standard [5].

Tensile properties at quasi-static rates are presented in section 3.1. Results in compression at quasi-static and high strain rates are presented in section 3.2. The strain rate sensitivity is calculated from the compressive results and presented in section 3.4. Numerical modelling to obtain parameters of the material constitutive equations based on results from a proprietary method are presented in section 3.5.

2 Experimental methods

The OFE copper used in this study was supplied by CERN. Sheets of 1, 2, and 4 mm in thickness were annealed at 600 °C for two hours under vacuum. Cylindrical specimens with a diameter of 8 mm, used in the split Hopkinson and quasi-static compression tests, were extracted from the 4 mm sheet by water jet cutting. Tensile specimens were cut from the same sheet, while 1

and 2 mm thick specimens were produced for an in-house high strain rate characterization technique.

Split Hopkinson pressure bar (SHPB) tests were performed at the Institut de Recherche Dupuy de Lôme (IRDL) of the Ecole Nationale Supérieure de Techniques Avancées (ENSTA) Bretagne. Different striker pressures, from 2.50 to 5.07 bar, yielding strain rates between 2,200 and 4,600 s^{-1}, were used. A total of 12 SHPB tests were performed at 6 different strain rates. Figure 1 shows the apparatus used for the SHPB tests. Striker, input and output bars made of maraging steel were used for the compression of the copper specimens. Quasi-static compression tests were performed on a screw-driven Instron® 5969 universal testing machine at a constant crosshead speeds of 0.5, 5, 50, and 250 mm/min, corresponding to nominal strain-rates from 2.11 x 10^{-3} to 1.05 s^{-1}. The strain was measured by image tracking of the displacement of the fixtures. To ensure repeatability, a minimum of two tests were performed for each condition in compression and tension, at both low and high strain rates.

Tensile tests were performed at crosshead speeds of 1 to 100 mm/min, at the IRDL, using a UTS screw-driven universal testing machine. The strain was measured in the gage section using an extensometer capable of large vertical displacements, see image on the right in Figure 1.

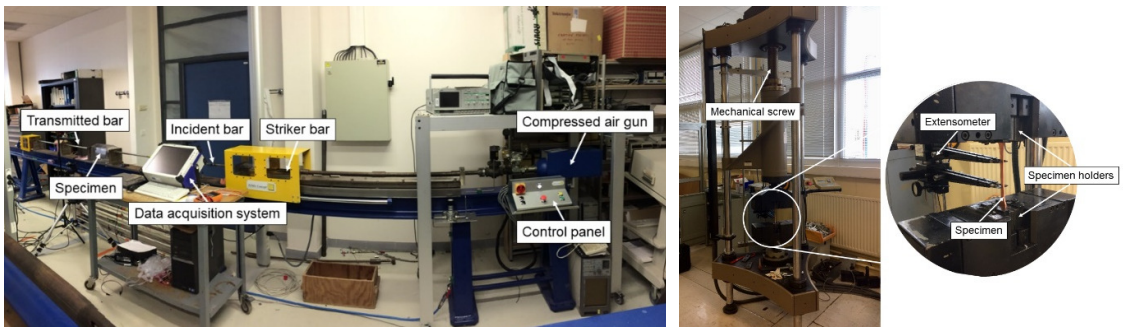

Figure 1: Left: Split Hopkinson setup used at the IRDL, ENSTA Bretagne. Right: Universal testing machine and extensometer used for the tensile tests.

Finally, in-house proprietary tests were performed at I-Cube Research. During this test, specimens are expanded at high velocity using electromagnetic forces and a photo Doppler velocimeter (PDV) probe is used to measure the velocity of the moving surface. The mechanical properties of the material are then determined using finite element models by identifying constitutive law parameters for which the experimental and numerical velocities are in agreement. The characterization method is similar to that of tube and ring expansion tests [6]–[8]. Due to the confidential nature of the test, no additional details are provided.

3 Results and discussion

3.1 Mechanical properties in tension at low strain rates

The tensile quasi-static properties were measured at four different strain rates in tension. To assess anisotropic properties of the blank, specimens were pulled parallel and perpendicular to the sheet's rolling direction. No significant difference in the uniaxial properties are observed for quasi-static strain rates at two different orders of magnitude, see Figure 2. Note that the plots

for the longitudinal (L) and transversal (T) directions are presented, where longitudinal specimens are pulled in the rolling direction of the sheet.

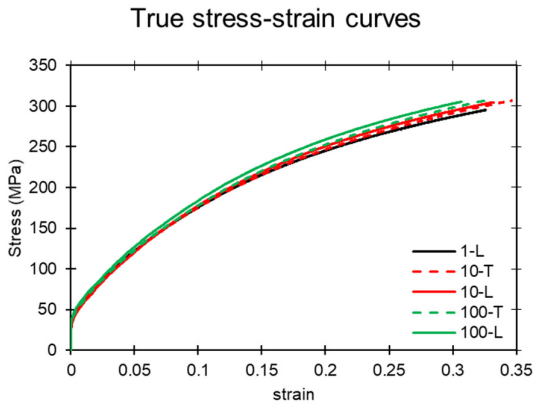

Figure 2: True stress-strain curves of uniaxial tensile specimens in longitudinal and transverse directions for three different crosshead speeds: 1, 10 and 100 mm/min (corresponding to initial strain rates in the gauge section of 2.4×10^{-4}, 2.4×10^{-3} and 2.4×10^{-2} s^{-1}.

Comparison of the strain hardening exponent, extracted from the Hollomon parabolic hardening equation ($\sigma = K\varepsilon^n$), the ultimate tensile strength (UTS) and the strain at fracture for the different strain rates also indicate a small strain rate sensitivity at quasi-static rates. The low effect of strain rate on the mechanical properties has previously been observed for annealed FCC metals, such as Al1050 [9].

3.2 Mechanical properties in compression at low and high strain rates

Quasi-static compressive tests were performed at four different strain rates, from 2.11×10^{-3} to 1.05 s^{-1}. Figure 3 shows the true stress-strain curves with one specimen per strain rate. A small increase in hardening rate is visible for increasing strain rate. The results of the compressive quasi-static tests are used for comparison with the mechanical properties obtained with compressive split Hopkinson bars, where specimens were deformed at around 4000 s^{-1}, up to six orders of magnitude greater.

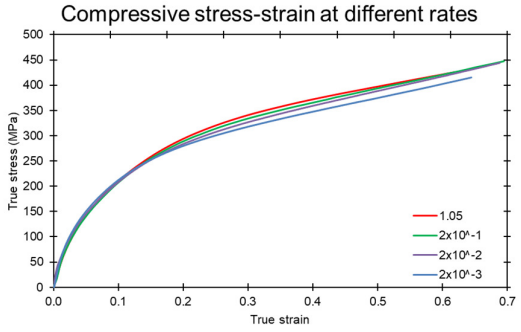

Figure 3: True stress-strain curves of compressive quasi-static tests of OFE-Cu for four different strain-rates: 2.11×10^{-3}, 2.11×10^{-2}, $2.11 \times 10^{-1}$and 1.05 s^{-1}.

Figure 4 compares the mechanical response of copper observed during uniaxial tensile and compressive tests performed at similar strain rates in the order of 2×10^{-3} and 2×10^{-2} s^{-1}. A slight difference in mechanical properties appears at the lower strain rate and is greater at 10^{-2} s^{-1}.

Note that the elastic regime is more apparent in the tensile results, where an extensometer was used.

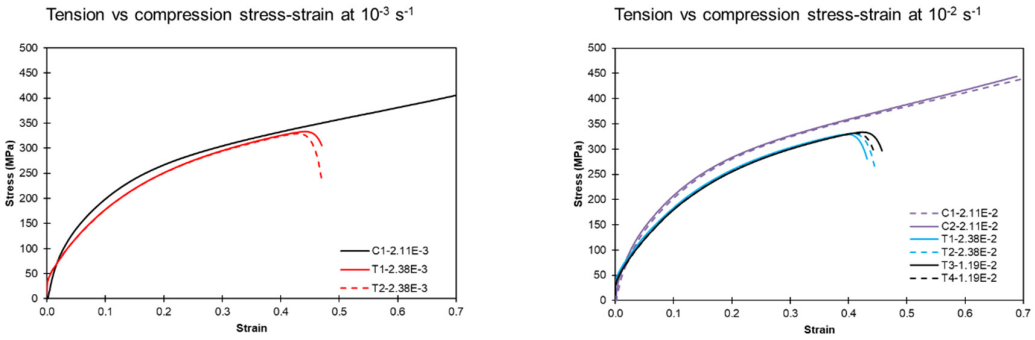

Figure 4: Comparison of the true stress-strain curves for tensile and compressive tests at strain rates in the order of 2×10^{-3} and 2×10^{-2} s^{-1}.

The theories behind split Hopkinson bars have been extensively reviewed in literature, e.g. by Gray III in a review paper [10] and Chen et al. in a textbook [11]. The reader is invited to consult review papers and textbooks on the subject to gain a deeper understanding on the matter.

Equilibrium of the stress state in a sample during the SHPB tests was verified with the one- and three-wave stress analyses and it was reached at a strain of around 0.15. This value agrees with the literature, where Gray III [10] supports that the first 10% of strain in SHPB tests cannot be used since the equilibrium condition has not been met. Moreover, an approximation of the rise time in a specimen, based on the average stage II work hardening of all the tests, was calculated and found equal to approximately 35 µs. Since the measured rise time of the transmitted wave is similar to the calculated rise time in the specimen, equilibrium of the stress state is again confirmed. The above verifications allow the calculation of the true stress using the back stress, which produces less noisy plots, using equations based on the assumption of a uniform strain wave passing through the specimen. Since the plastic deformation starts at a strain lower than 0.15, the initial yield stress cannot be measured in the high strain-rate tests.

Stress strain curves of the OFE-Cu specimens at six different strain rates, between 2249 and 4213 s^{-1} are presented in Figure 5. To confirm the trend of the experimental curves and the stress and strain values obtained, a comparison was made with results reported in literature on copper with similar composition and heat treatments [12]. Mechanical properties of Oxygen Free High Conductivity (OFHC) Cu in compression at 3000 s^{-1} published by Bodelot et al. showed similar mechanical properties [12]. The difference in properties is expected to arise from the different heat treatments used in Bodelot's work: (1) 600 °C - 1 h, (2) 800 °C - 1 h and (3) 900 °C - 35 min, and the different composition of the copper specimens. Recall that the OFE-Cu used in this study was heat treated at 600 °C for 2 h, under vacuum. The strain hardening rates are similar and the stress at corresponding strains is higher for the experimental results on OFE-Cu, always with less than 25% of difference.

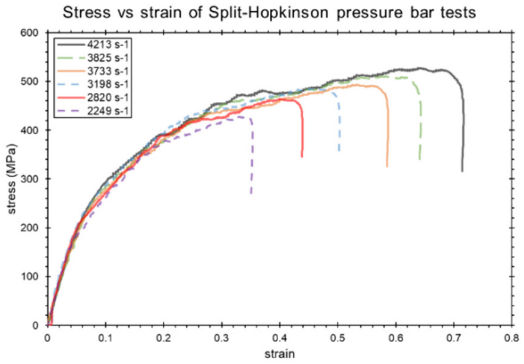

Figure 5 : SHPB stress-strain results at different strain rates for annealed OFE-Cu.

From Figure 5, an increase in the flows stress (at a given strain) is hardly noticeable for increasing strain rates. Significant differences in mechanical properties are usually noticeable for strain rates that are different by one order of magnitude. The comparison with the quasi-static compression tests performed at a strain rate three to six orders of magnitude lower are then of interest.

3.3 Comparison of split Hopkinson and quasi-static compressive tests

As reported in literature by Gray III [13] , Nemat-Nasser [14] and others, an increase of the apparent strain hardening rate and similar initial yield stress for increasing strain rate is observed in annealed FCC metals. It is clear from the compression curves at low and high strain rates, see Figure 6, that strain hardening significantly increased.

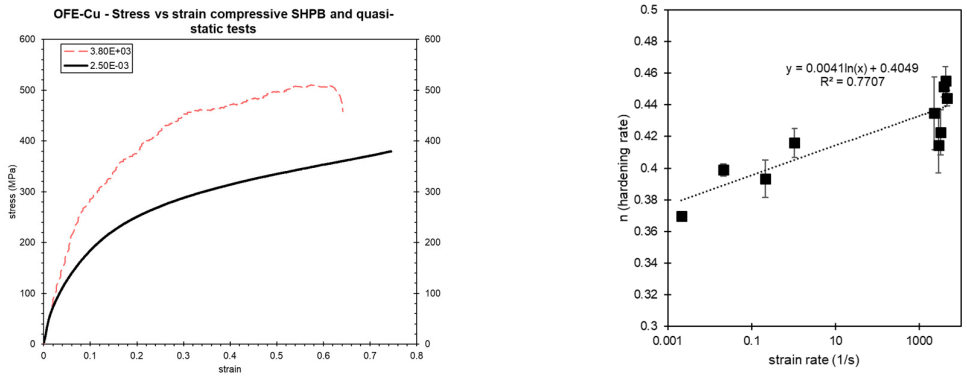

Figure 6: Left: Compressive true stress-strain curves from split Hopkinson (3,800 s^{-1}) and quasi-static tests (2.5×10^{-3} s^{-1}). Right: Evolution of the apparent strain hardening exponent with strain-rate, from the quasi-static and split Hopkinson compressive tests.

The natural logarithm of the flow stress and plastic strain of all quasi-static and dynamic curves were plotted and a linear fit was used to quantify the increase in strain hardening rate. The slope of each linear curve corresponds to the strain hardening exponent, (n), from the Hollomon parabolic strain-hardening equation. Figure 6 depicts the increase in strain hardening exponent for the specimens compressed at different strain rates. The linear trend of the semi-log plot indicates a logarithmic dependency of the strain hardening exponent with the strain rate. This explains the previous statement that a difference in the mechanical properties is mainly observed between specimens strained with an order of magnitude of difference in strain rate.

A similar comparison of the properties at low and high strain rates in compression was performed by Nemat-Nasser et al. [14] on annealed OFHC copper at different temperature and at strain rates of 8000 and 0.001 s^{-1}. The increase in hardening rate experimentally observed is confirmed from comparison with the OFHC-Cu results of the literature.

It is of interest to note the higher mechanical properties of OFE-Cu used during this study compared witht the OFHC-Cu used by Bodelot et al. [12] and Nemat-Nasser et al. [14]. The small difference in material composition and heat treatments are suspected to be reponsible for this observation. The difference with the literature, in absolute values and not trends, justifies the need of this study to properly characterize the OFE copper sheets used to form SRF cavities for particle accelerators.

3.4 Strain rate sensitivity

The strain rate sensitivity of metals is defined by evaluating the relationship between flow stress and the strain rate. Such an analysis is performed, and results are compared with the literature. Figure 7 shows the strain rate sensitivity plot where the flow stress is plotted as a function of the logarithm of the strain rate for a true strain of 15%, to allow a comparison with literature. An apparent increase in strain sensitivity is observed around 10^3 s^{-1}. A similar behavior was also observed by Follansbee et al. [15], see Figure 7. Different hypotheses have been formulated to explain the substantial increase in flow observed at high-strain rates in FCC metals: viscous drag effects [16], [17], and the dependence on strain-rate of the microstructure evolution [15], [18].

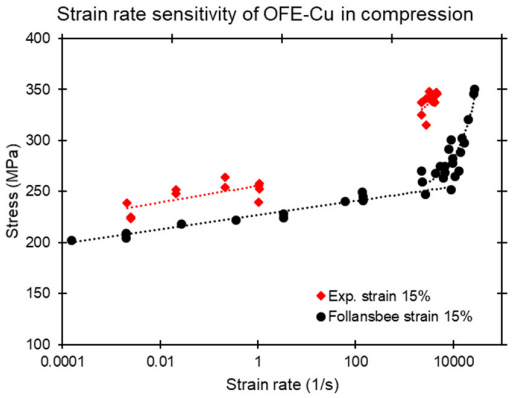

Figure 7: Strain rate sensitivity of annealed OFE-Cu at 15% strains compared with previous results of Follansbee et al. [15].

3.5 Numerical modelling

During electro-hydraulic forming of SRF cavities, the blank experiences high compressive stresses through its thickness from impacts with the die at high speed and tensile stresses from the expansion into the final geometry. To characterize the material properties of OFE-Cu at different strain rates based on a constitutive equation, a combined experimental-numerical approach is employed. This process is done iteratively using the LS-OPT optimization software coupled with LS-DYNA that solves finite element models for different loading scenarios. Figure 8 shows a flowchart of the process used to identify adequate material parameters. For

the split Hopkinson compressive tests, experimental and numerical stress histories in the specimen are compared. For the proprietary test (using electromagnetic forces), velocity-time curves are compared. The convergence of the results to the most accurate solution is accessed based on the mean squared error of the properties in the y axis, i.e. stress or velocity. Both Johnson-Cook (JC) and Zerilli-Armstrong (ZA) constitutive equations were considered, but results are only presented for JC since ZA curve fittings were not representative of the experimental results.

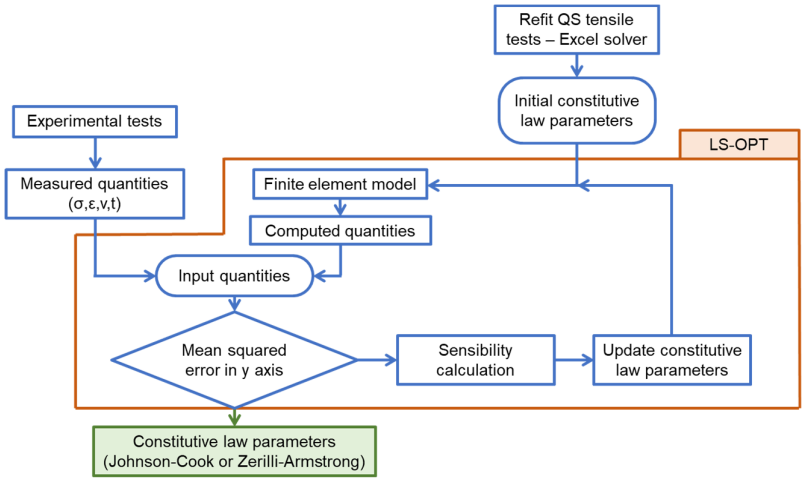

Figure 8: Flowchart of the sequence combining experimental tests and finite element models to identify the optimal constitutive law parameters.

Most materials have mechanical properties that are dependent on the applied strain rate. Additionally, temperature rise in materials from the conversion of strain energy into heat can be significant at high strain rates. Constitutive equations with strain rate and temperature dependencies are then required for finite element codes to predict the behavior of a deforming blank. Some constitutive equations are purely empirical, such as the JC model [19], while other constitutive equations, such as the ZA model, are based on dislocation mechanics [20]. The JC model is often used in dynamic applications due to its simplicity and its low number of parameters to identify. The strain rate has a logarithmic proportionality with the flow stress, while the thermal softening is dependent on a reference temperature and the melting point of the metal [21]. The JC model is defined by the following equation:

$$\sigma = (A + B\varepsilon_p^n)\left(1 + C\ln\frac{\dot{\varepsilon}}{\dot{\varepsilon}_0}\right)(1 - (T^*)^m) \quad (1)$$

where A, B, n, C and m are material constants determined empirically, ε_p is the plastic strain, $\dot{\varepsilon}$ is the strain rate in s^{-1}, $\dot{\varepsilon_0}$ is the reference strain rate, often fixed at 1, in s^{-1}, $T^* = \frac{T-T_0}{T_m-T_0}$ is the thermal softening term, where T, T_0 and T_m are the temperatures of the specimen, at a reference state, often room temperature, and the melting point, respectively, all in K. Note that the Johnson-Cook formulation in LS-DYNA defines $\dot{\varepsilon}_0$ as the threshold strain rate at which rate effects are present [22].

Since parameters A, B and n are only strain dependent and all quasi-static tests showed no significant differences in mechanical properties, the identification of those three parameters is

performed using only quasi-static results. Moreover, since no significant rate-sensitivity was observed during the quasi-static tests, the threshold strain rate is fixed to $1\ \mathrm{s}^{-1}$. Assuming the process is isothermal, the JC equation is simplified as follow for the quasi-static tests:

$$\sigma = A + B\varepsilon_p^n \tag{2}$$

Identification of A, B and n is performed with the *Solver* function of Excel, based on the mean-square error between experimental and calculated stresses. Figure 9 shows the stress-strain curves derived from equation 2 with parameters identified using low strain rate tensile and compressive results. Values of the parameters are presented in Table 1. A lower strain hardening rate is visible for the JC parameter identified in compression, aligning with the experimental results in Figure 4.

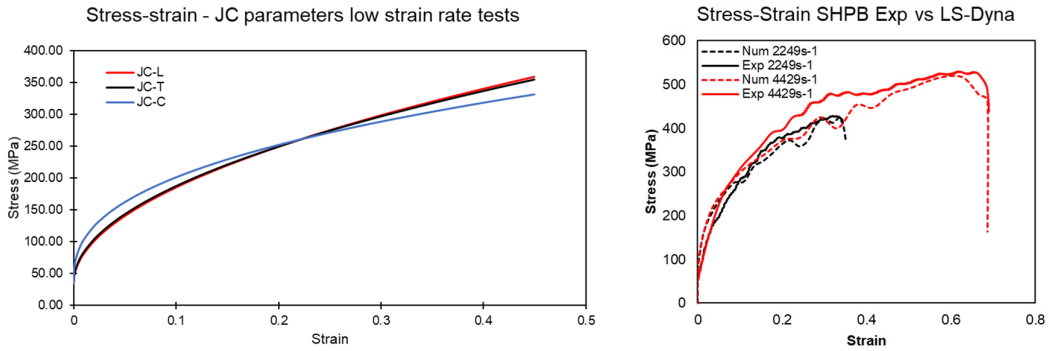

Figure 9: Left: Stress-strain curves with the simplified Johnson-Cook equation for tensile tests in the longitudinal and transversal directions (JC-L and JC-T, respectively) and for compressive tests (JC-C). Right: Stress-strain curves comparison between numerical models and experimental results for the lowest and highest strain rates obtained during the SHPB tests.

The identification of the strain rate and temperature dependent constants, respectively C and m, is performed using LS-OPT and LS-DYNA. For the compressive parameters, a 2D (axisymmetric) explicit numerical model of the split Hopkinson test is used. The experimental velocity of the face of the input bar in contact with the specimen is used as an input to the finite element code. Stress and strain values in the modelled specimen are extracted for comparison with experimental curves, see Figure 9, and parameter identification. For the tensile parameters, a 3D explicit numerical model of the proprietary test deforming specimens at high velocity using electromagnetic forces is used. Note that this test does not deform specimen in pure tension, but with a multitude of bending stress waves propagating in the specimen. The velocity of the external face of the specimen is extracted from the numerical model and compared with experimental results. Experiment were performed at different discharge voltages, yielding strain rates of up to 2000 s^{-1}. The sets of material parameters obtained from the optimization procedure are given in Table 1.

Table 1: Johnson-Cook parameters identified from tensile and compressive tests.

Parameter	Proprietary and tensile tests	SHPB and compression tests
A (MPa)	34.25	34.25
B (MPa)	487.47	403.78
n	0.5102	0.3845

C	0.09	0.09
m	1.2	1.2

It is interesting to noticed that the same set of strain-rate and temperature dependent parameters (C and m) were identified for the tensile and compressive tests. This finding confirms that the in-house test is reliable for the identification of Johnson-Cook parameters for FCC materials deformed in tension, benchmarked with a standardized test in pure compression.

4 Conclusion

Parameters for the Johnson-Cook equation were identified in tension and compression for annealed oxygen-free electronic copper based on compression and tensile quasi-static tests, a proprietary test at high rate in tension, and split Hopkinson compression tests. The values of the constitutive law's constants in both stress states were similar and no anisotropic properties were measured in tension.

Additional, split Hopkinson tests in tension should be performed in the upcoming months to validate the Johnson-Cook parameters and to verify if the difference in mechanical properties between compression and tension observed at quasi-static rates is present at high strain-rates.

It will be also interesting to consider other constitutive models for the identification procedure.

Using the identified parameters, simulations of electro-hydraulic forming operations of copper parts will be performed and compared to available experimental data.

Acknowledgement

The authors would like to thank the European Advanced Superconductivity Innovation and Training (EASITrain) program for the financial support. This Marie Sklodowska-Curie Action (MSCA) Innovative Training Networks (ITN) has received funding from the European Union's H2020 Framework Programme under grant agreement no. 764879.

The authors would also like to the thank Dr. Carolina Abajo Clemente and Said Atieh of CERN's MME group for the supply of the material characterized in this study.

The authors would also like to thank all employees of I-Cube Research that helped on various tasks for this work.

References

[1] "Future Circular Collider Study. Volume 2: The Lepton Collider (FCC-ee) Conceptual Design Report, preprint edited by M. Benedikt et al. CERN accelerator reports, CERN-ACC-2018-0057," Geneva, Dec. 2018.

[2] "Future Circular Collider Study. Volume 3: The Hadron Collider (FCC-hh) Conceptual Design Report, preprint edited by M. Benedikt et al. CERN accelerator reports, CERN-ACC-2018-0058," Geneva, Dec. 2018.

[3] "International collaboration publishes concept design for a post-LHC future circular collider at CERN," *CERN*. [Online]. Available: https://home.cern/news/press-release/accelerators/international-collaboration-publishes-concept-design-post-lhc. [Accessed: 12-Feb-2019].

[4] E. Cantergiani *et al.*, "Niobium superconducting rf cavity fabrication by electrohydraulic forming," *Phys. Rev. Accel. Beams*, vol. 19, no. 11, Nov. 2016.

[5] ASTM International, "ASTM B170-99(2015), Standard Specification for Oxygen-Free Electrolytic Copper—Refinery Shapes," West Conshohocken, PA, 2015.

[6] A.-C. Jeanson *et al.*, "Identification du comportement mécanique dynamique de métaux par un essai d'expansion électromagnétique de tube," presented at the 11ème Colloque National en Calcul des Structures, 2013.

[7] A.-C. Jeanson *et al.*, "Identification of Material Constitutive Parameters for Dynamic Applications: Magnetic Pulse Forming (MPF) and Electrohydraulic Forming (EHF)," p. 7, 2014.

[8] A.-C. Jeanson, F. Bay, N. Jacques, G. Avrillaud, M. Arrigoni, and G. Mazars, "A coupled experimental/numerical approach for the characterization of material behaviour at high strain-rate using electromagnetic tube expansion testing," *Int. J. Impact Eng.*, vol. C, no. 98, pp. 75–87, 2016.

[9] K. Higashi, T. Mukai, K. Kaizu, S. Tsuchida, and S. Tanimura, "Strain Rate Dependence on Mechanical Properties in some Commercial Aluminum Alloys," *J. Phys. IV Colloq.*, vol. 01, no. C3, pp. C3-341-C3-346, 1991.

[10] G. T. (Rusty) Gray, "High-Strain-Rate Testing of Materials: The Split-Hopkinson Pressure Bar," in *Characterization of Materials*, E. N. Kaufmann, Ed. Hoboken, NJ, USA: John Wiley & Sons, Inc., 2012.

[11] W. W. Chen and B. Song, *Split Hopkinson (Kolsky) bar: design, testing and applications*. New York, NY: Springer, 2011.

[12] L. Bodelot *et al.*, "Microstructural changes and in-situ observation of localization in OFHC copper under dynamic loading," *Int. J. Plast.*, vol. 74, pp. 58–74, Nov. 2015.

[13] G. T. (Rusty) Gray, "High-Strain-Rate Deformation: Mechanical Behavior and Deformation Substructures Induced," *Annu. Rev. Mater. Res.*, vol. 42, no. 1, pp. 285–303, Aug. 2012.

[14] S. Nemat-Nasser and Y. Li, "Flow stress of f.c.c. polycrystals with application to OFHC Cu," *Acta Mater.*, vol. 46, no. 2, pp. 565–577, Jan. 1998.

[15] P. S. Follansbee and U. F. Kocks, "A constitutive description of the deformation of copper based on the use of the mechanical threshold stress as an internal state variable," *Acta Metall.*, vol. 36, no. 1, pp. 81–93, Jan. 1988.

[16] A. Kumar and R. G. Kumble, "Viscous Drag on Dislocations at High Strain Rates in Copper," *J. Appl. Phys.*, vol. 40, no. 9, pp. 3475–3480, Aug. 1969.

[17] F. J. Zerilli and R. W. Armstrong, "The effect of dislocation drag on the stress-strain behavior of F.C.C. metals," *Acta Metall. Mater.*, vol. 40, no. 8, pp. 1803–1808, Aug. 1992.

[18] A. Molinari and G. Ravichandran, "Constitutive modeling of high-strain-rate deformation in metals based on the evolution of an effective microstructural length," *Mech. Mater.*, vol. 37, no. 7, pp. 737–752, Jul. 2005.

[19] G. R. Johnson and W. H. Cook, "A constitutive model and data for metals subjected to large strains, high strain rates and high temperatures." 1983.

[20] F. J. Zerilli and R. W. Armstrong, "Dislocation-mechanics-based constitutive relations for material dynamics calculations," *J. Appl. Phys.*, vol. 61, no. 5, pp. 1816–1825, Mar. 1987.

[21] M. A. Meyers, *Dynamic behavior of materials*. New York, NY: Wiley, 1994.

[22] LSTC, "LS-DYNA® Keyword user's manual – Volume II, LS-DYNA R9.0." 2016.